International Journal of Power Electronics and Drive System (IJPEDS)
Vol. 17, No. 1, March 2026, pp. 414~424
ISSN: 2088-8694, DOI: 10.11591/ijpeds.v17.i1.pp414-424

A novel hybrid PI and adaptive super-twisting sliding mode controller for high-performance integrated speed and flux regulation of IMDs

Duc Thuan Le, Ngoc Thuy Pham
Department of Electrical Engineering Technology, Industrial University of Ho Chi Minh City, Ho Chi Minh City, Vietnam

Article Info

Article history:

Received Sep 8, 2025
Revised Jan 26, 2026
Accepted Feb 15, 2026

Keywords:

Adaptive super-twisting sliding mode
Field-oriented control
Hybrid PI control
Induction motor drives
Nonsingular terminal sliding mode control

ABSTRACT

This paper presents a novel hybrid control strategy that integrates a proportional–integral (PI) regulator with an adaptive super-twisting sliding mode controller (ASTA) defined on a nonsingular terminal sliding mode control (NTSMC) surface for high-performance induction motor drives (IMDs). This enhanced hybrid PI–ASTA–NTSMC architecture jointly exploits the steady-state accuracy of PI control and the finite-time robustness of a higher-order sliding mode formulation. The adaptive mechanism of the super-twisting algorithm dynamically adjusts the switching gains according to the instantaneous sliding variable, ensuring consistent performance under time-varying loads and parameter variations. The NTSMC surface guarantees singularity-free finite-time convergence, while the adaptive ASTA law suppresses chattering and enhances disturbance rejection. Simulation results across multiple operating conditions show that the proposed controller significantly outperforms PI and PI–FOSMC schemes. It achieves the fastest transient, reducing settling time to 0.0407 s (39.4% and 31.5% faster than PI and PI–FOSMC), with overshoot lowered to 0.0091 rad/s and ISE/IAE minimized to 0.0035 and 0.0256, confirming its superior tracking precision. Additionally, reductions in the speed and torque RMSE indicate smoother control effort and improved closed-loop performance. The Lyapunov-based analysis confirms global finite-time stability of the overall system. With its enhanced robustness, low sensitivity to sampling noise, and continuous higher-order sliding structure that suppresses chattering, the proposed hybrid PI–ASTA–NTSMC offers a computationally efficient and practically attractive solution for integrated speed–flux control in industrial IM drives.

Corresponding Author:

Duc Thuan Le
Department of Electrical Engineering Technology, Industrial University of Ho Chi Minh City
Ho Chi Minh City, Vietnam
Email: leducthuan@iuh.edu.vn

1. INTRODUCTION

Induction motors (IMs) are widely utilized in industrial drive systems owing to their robustness, simple mechanical structure, and low manufacturing cost. Despite these advantages, achieving precise and robust regulation of both speed and flux remains a critical challenge in high-performance applications, particularly under parameter uncertainties, load disturbances, and external perturbations. Since its introduction in the 1970s [1], field-oriented control (FOC) has become the cornerstone of IM drives, providing decoupled control of torque and flux, fast transient response, and reliable steady-state performance over wide operating ranges. In conventional FOC schemes, the outer speed and inner flux control loops are typically implemented using proportional–integral (PI) controllers due to their straightforward structure and ease of tuning. However, the fixed-gain nature of PI regulators makes them highly sensitive to motor parameter variations and external disturbances. Consequently, conventional PI-based control often results in performance degradation such as overshoot, long settling time, and poor steady-state precision under dynamic operating conditions [2]–[5].

To enhance performance and robustness, several hybrid PI-based control strategies have been developed by combining PI regulators with intelligent or nonlinear techniques. For instance, PI–fuzzy logic controllers (PI–FLCs) employ fuzzy inference to adaptively adjust PI gains, improving transient and steady-state performance [6], [7]. Likewise, PI–artificial neural network (PI–ANN) and PI–radial basis function (PI–RBF) schemes utilize learning mechanisms to handle system nonlinearities and parameter uncertainties [8]–[10]. Although these intelligent hybrid controllers exhibit superior adaptability, they often entail high computational cost, complex design processes, and lack rigorous theoretical stability guarantees factors that hinder their practical industrial adoption. Among robust nonlinear control techniques, sliding mode control (SMC) has attracted considerable attention due to its inherent robustness against parameter variations, external disturbances, and unmodeled dynamics [11]–[13]. The classical first-order SMC (FOSMC) ensures strong robustness under matched uncertainties but suffers from chattering, which may excite unmodeled high-frequency dynamics and cause mechanical wear [14], [15]. To alleviate this issue, higher-order SMC (HOSMC) approaches such as the super-twisting algorithm (STA) have been developed, offering finite-time convergence with significantly reduced chattering [16]–[20]. Meanwhile, advancements in sliding surface design have introduced terminal sliding mode control (TSMC) and nonsingular terminal SMC (NTSMC) formulations. While TSMC achieves finite-time convergence, it suffers from a singularity near the equilibrium point. In contrast, the NTSMC formulation eliminates this singularity, ensuring bounded control effort and robust finite-time convergence [21]–[27].

Unlike previous hybrid PI–SMC schemes, this paper introduces an entirely new hybrid configuration that integrates nonsingular terminal dynamics with higher-order continuous control action, thereby unifying finite-time convergence without singularity and ensuring enhanced smoothness in the control response. The ASTA–NTSMC component guarantees rapid finite-time convergence, superior robustness against parameter variations and external disturbances, and smooth control effort owing to the higher-order continuity of the super-twisting algorithm. The PI component, on the other hand, preserves steady-state accuracy and allows intuitive gain tuning, maintaining industrial simplicity and practical implementation feasibility. Moreover, the proposed adaptive mechanism dynamically adjusts the switching gains of the STA law in accordance with the instantaneous sliding dynamics, significantly improving the controller’s robustness and adaptability under time-varying operating conditions.

Additionally, the hybrid PI–ASTA–NTSMC structure is also employed for the flux control loop, forming an integrated dual-loop architecture that achieves superior torque smoothness, flux stability, and overall drive efficiency. The global stability and robustness of the proposed controller are rigorously established through Lyapunov-based analysis, confirming the finite-time convergence of the closed-loop IM drive system. The major contributions of this paper are summarized as follows: i) A novel hybrid PI–ASTA–NTSMC control strategy is developed for FOC-based IM drives, enabling integrated speed and flux regulation with steady-state precision, finite-time convergence, and adaptive robustness within a unified framework; ii) A Lyapunov-based stability analysis is presented to rigorously establish global finite-time convergence of the closed-loop system under parameter variations and external disturbances; and iii) Comprehensive simulations under wide-speed operation, load torque disturbances, and parameter uncertainties quantitatively demonstrate the superiority of the proposed controller over conventional PI and PI–FOSMC schemes.

The remainder of this paper is organized as follows: i) Section 2 reviews the fundamental principles of FOC for IM drives; ii) Section 3 details the proposed hybrid PI–ASTA–NTSMC controller and its stability analysis; iii) Section 4 presents simulation results and comparative evaluations; and iv) Finally, section 5 concludes the paper with key findings and directions for future work.

2. MATHEMATICAL MODEL OF IMDs

The induction motor (IM) model in the synchronously rotating reference frame, serving as the foundation of field-oriented control (FOC), is expressed in state-space form as (1) [28].

$$\dot{x}(t) = Ax(t) + Bu(t) \tag{1}$$

Where: x, A, B, and u are state vectors, state matrix, input matrix, control input, and they can be defined as:

$$x(t) = [i_{s\alpha} \quad i_{s\beta} \quad \varphi_{r\alpha} \quad \varphi_{r\beta} \quad \omega_r]^T \; u(t) = [u_{s\alpha} \quad u_{s\beta} \quad T_L]^T$$

$$A = \begin{bmatrix} a_{11} & 0 & a_{13} & a_{14} & a_{15} \\ 0 & a_{11} & -a_{14} & a_{13} & a_{25} \\ \frac{L_m}{\tau_r} & 0 & \frac{-1}{\tau_r} & \omega_r & \varphi_{r\beta} \\ 0 & \frac{L_m}{\tau_r} & -\omega_r & \frac{-1}{\tau_r} & -\varphi_{r\alpha} \\ -b\varphi_{r\beta} & b\varphi_{r\alpha} & bi_{s\beta} & -bi_{s\alpha} & \left(\frac{-B}{J}\right) \end{bmatrix} B = \begin{bmatrix} \frac{1}{\sigma L_s} & 0 & 0 \\ 0 & \frac{1}{\sigma L_s} & 0 \\ 0 & 0 & 0 \\ 0 & 0 & 0 \\ 0 & 0 & \frac{-1}{J} \end{bmatrix}$$

With $i_{s\alpha}$; $i_{s\beta}$; $u_{s\alpha}$; $u_{s\beta}$; $\varphi_{r\alpha}$; $\varphi_{r\beta}$ are components of the stator's current, stator's voltage, and rotor's flux in the $\alpha\beta$ reference frame. *Te*, T_L: electromagnetic and load torque; respectively; ω_r: the angular velocity (mechanical speed), $\omega_r = (2/P)\omega_{re}$; ω_{re}, ω_{sl}, ω_e: the electrical speed, respectively rotor and slip angular and synchronous angular velocity; *p*: number of pole pairs. *Ls*, *Lr*: stator and rotor inductances; *Lm*: mutual inductance; *Rs*, *Rr*: stator and rotor resistances; *J*: the inertia of motor and load; σ: total linkage coefficient; *B*: friction coefficient; and τ_r: rotor time constant.

Based on the dynamics of IM in the stator fixed reference frame, the stator flux can be estimated such as:

$$\tau_r = \frac{L_r}{R_r};\ \sigma = 1 - \frac{L_m^2}{L_r L_s};\ \gamma = \frac{L_m}{L_r};\ k = \frac{3pL_m}{2L_r};\ b = \frac{k}{J}$$

$$a_{11} = -\frac{1}{\sigma L_s}\left(R_s + \frac{L_m^2}{L_r\tau_r}\right);\ a_{13} = \frac{\gamma}{\sigma L_s \tau_r};\ a_{14} = -\frac{\gamma}{\sigma L_s}\omega_r;\ a_{15} = -\frac{\gamma}{\sigma L_s}\varphi_{r\beta};\ a_{25} = \frac{\gamma}{\sigma L_s}\varphi_{r\alpha}$$

The electromagnetic torque and the slip frequency can be expressed in the dq reference frame:

$$\begin{cases} \varphi_{s\alpha} = \int_0^t (u_{s\alpha} - R_s i_{s\alpha})dt \\ \varphi_{s\beta} = \int_0^t (u_{s\beta} - R_s i_{s\beta})dt \end{cases} \tag{2}$$

The stator and rotor flux linkage phase is given by (3).

$$\varphi_s = \sqrt{\varphi_{s\alpha}^2 + \varphi_{s\beta}^2};\quad \varphi_r \approx \frac{L_m}{L_r}\varphi_s \tag{3}$$

Torque can be calculated as (4).

$$T_e = \frac{3}{2}p\left(i_{s\beta}\varphi_{s\alpha} - i_{s\alpha}\varphi_{s\beta}\right) \tag{4}$$

The mechanical dynamics follow:

$$J\frac{d\omega_r}{dt} = T_e - T_L - B\omega_r \tag{5}$$

3. NOVEL HYBRID PI–ASTA-NTSM STRATEGY

3.1. Speed control strategy

This subsection introduces the proposed adaptive PI–ASTA–NTSMC speed control framework for induction motor drives. The controller integrates a conventional PI regulator with an adaptive super-twisting algorithm designed on a nonsingular terminal sliding mode control surface. Within this hybrid structure, the PI regulator ensures steady-state accuracy and control simplicity, while the NTSMC-based surface guarantees finite-time convergence and eliminates the singularity issues of conventional TSMC.

The adaptive mechanism embedded in the STA law continuously adjusts the switching gains in real time according to the instantaneous sliding dynamics. This self-tuning feature enables the controller to maintain optimal performance under parameter variations, load disturbances, and time-varying operating conditions, without requiring prior knowledge of uncertainty bounds. Consequently, the proposed controller simultaneously achieves high robustness, improved adaptability, and effective chattering suppression.

Compared with conventional PI and PI–FOSMC approaches, the proposed method offers four major advantages: i) faster transient response and shorter settling time, ii) reduced overshoot and torque ripple, iii) adaptive robustness against parameter and load variations, and iv) enhanced steady-state precision with minimized chattering effects. The proposed control strategy, therefore, ensures smooth electromagnetic torque, reduced mechanical stress, and high dynamic reliability, providing a practical high-performance solution for industrial IM drive systems. Based on this structure, the tracking errors are defined as (6).

$$e_\omega(t) = \omega_r^*(t) - \omega_r(t) \tag{6}$$

To guarantee finite-time convergence and avoid singularities, the proposed sliding surface is defined as (7).

$$s_\omega(t) = e_\omega(t) + \alpha_1 |e_\omega(t)|^{p/q} sat\left(\frac{e_\omega(t)}{\phi}\right); With:\ \alpha_1 > 0;\ \phi > 0\ \&\ 0 < \frac{p}{q} < 1 \tag{7}$$

The derivative of the sliding surface is given by (8).

$$\dot{s}_\omega(t) = \dot{e}_\omega(t) + \alpha_1 \frac{p}{q} |e_\omega(t)|^{(p/q)-1} sat\left(\frac{e}{\phi}\right) + \alpha |e|^{(p/q)} \frac{d}{dt}\left[sat\left(\frac{e_\omega(t)}{\phi}\right)\right] \tag{8}$$

The Lyapunov function is selected as (9).

$$V_\omega(t) = \frac{1}{2} s_\omega^2(t) \tag{9}$$

Its derivative can obtain:

$$\frac{dV_\omega(t)}{dt} = s_\omega(t)\dot{s}_\omega(t) \tag{10}$$

To satisfy: $\frac{dV_\omega(t)}{dt} < 0$ then: $s_\omega(t)\dot{s}_\omega(t) < 0$. From (8), a hybrid PI + ASTA_NTSMC control law is designed as (11) and (12).

$$\dot{s}_\omega(t) = -\beta_1 u_\omega(t) = -\beta_1 \left[K_{p\omega} e_\omega(t) + K_{I\omega} \int_0^t e_\omega(t) dt + u_{\omega \mathrm{ASTA}}(t)\right] \tag{11}$$

$$u_{\omega \mathrm{ASTA}}(t) = \phi_\omega(s_\omega(t)) + v_\omega(t) \tag{12}$$

Where: $\begin{cases} \phi_\omega(s_\omega(t)) = k_{\alpha_1}(t)|s_\omega(t)|^{1/2} sat\left(\frac{s_\omega(t)}{\phi}\right) \\ v_\omega(t) = k_{\beta 1}(t) \int_0^t sat\left(\frac{s_\omega(t)}{\phi}\right) dt \end{cases}$. The virtual control vector i_{sq}^* is designed as (13).

$$i_{sq}^* = \frac{2L_r}{3pL_m\varphi_r}\{J\dot{\omega}_r^* + B\omega_r^* + T_L + \beta u(t)\} \tag{13}$$

3.2. Flux control strategy

Accurate rotor-flux regulation is essential for linear torque production, low torque ripple, and high efficiency in field-oriented induction motor drives. Conventional PI-based flux control degrades under parameter variations, magnetic saturation, inverter nonlinearities, and rapid load changes, leading to flux oscillations and reduced torque smoothness. To address these limitations, the flux loop in this work adopts the proposed hybrid PI–ASTA–NTSMC structure, which combines PI action with an adaptive super-twisting term on a nonsingular terminal sliding surface to achieve time-adaptive flux regulation with finite-time convergence and minimal chattering. The rotor flux is obtained from a current-model-based estimator. The resulting flux tracking error is defined as (14).

$$e_\varphi(t) = \varphi_r^*(t) - \hat{\varphi}_r(t) \tag{14}$$

Where $\varphi_r^*(t)$ denotes the reference flux and $\hat{\varphi}_r(t)$ is the estimated rotor flux. The hybrid PI–ASTA–NTSMC flux controller uses $e_\varphi(t)$ to generate the d-axis current reference, ensuring rapid, robust flux convergence while avoiding excessive control activity and steady-state oscillations. The sliding surface is designed according to the nonsingular terminal function:

$$s_\varphi(t) = e_\varphi(t) + \alpha_2 \left|e_\varphi(t)\right|^{p/q} sat\left(\frac{e_\varphi(t)}{\phi}\right); With:\ \alpha_2 > 0;\ \phi > 0\ \&\ 0 < \frac{p}{q} < 1 \tag{15}$$

The Lyapunov function is selected as (16).

$$V_\varphi(t) = \frac{1}{2} s_\varphi^2(t) \tag{16}$$

Its derivative can obtain:

$$\frac{dV_\varphi(t)}{dt} = s_\varphi(t)\dot{s}_\varphi(t) \tag{17}$$

to satisfy: $\frac{dV_\varphi(t)}{dt} < 0$ then: $s_\varphi(t)\dot{s}_\varphi(t) < 0$. Based on the derived sliding surface, the control law is designed as (18).

$$\dot{s}_\varphi(t) = -\beta_2 u_\varphi(t) = -\beta_2 \left[K_{p\varphi} e_\varphi(t) + K_{I\varphi} \int_0^t e_\varphi(t)dt + u_{\varphi \mathrm{AST}A}(t)\right] \tag{18}$$

Where: $u_{\varphi ASTA}(t) = \phi_\varphi\left(s_\varphi(t)\right) + v_\varphi(t)$; with: $\begin{cases} \phi_\varphi\left(s(t)\right) = k_{\alpha 2}(t)\left|s_\varphi(t)\right|^{1/2} sat\left(\frac{s_\varphi(t)}{\phi}\right) \\ v_\varphi(t) = k_{\beta 2}(t)\int_0^t sat\left(\frac{s_\varphi(t)}{\phi}\right)dt \end{cases}$

The virtual control vector isq is designed as (19).

$$i_d^*(t) = \frac{\tau_r}{L_m}\left[\frac{d\varphi_r^*}{dt} + \frac{1}{\tau_r}\varphi_r^* + K_{p\varphi} e_\varphi(t) + K_{I\varphi}\int_0^t e\varphi(t)dt + u_{\varphi \mathrm{AST}A}(t)\right] \tag{19}$$

3.3. Adaptive gain laws (ASTA gains) and Lyapunov stability analysis

The gains $k_{\alpha i}(t)$ and $k_{\beta i}(t)$are updated using an adaptive law of the form:

$$\dot{k}_{ij}(t) = \begin{cases} \delta_{ij}|s| + \gamma_{ij} k_{ij}(t-1), & k_{ij}(t) > k_{ij,min} \\ k_{ij,min} > 0, & otherwise \end{cases} (i = \alpha{:}\beta;\ j = 1{:}2) \tag{20}$$

Where $\delta_{ij} > 0$ and $\gamma_{ij} > 0$ are adaptation and damping coefficients, respectively. This rule ensures that the gains increase when the sliding variable deviates from zero (indicating larger uncertainty) and decrease smoothly when the system approaches equilibrium, thus balancing chattering suppression and disturbance rejection. The Lyapunov function is selected as (21).

$$V(t) = V_\omega(t) + V_\varphi(t) = \frac{1}{2}\left[s_\omega^2(t) + s_\varphi^2(t)\right] \tag{21}$$

Combining (10), (11), (17), and (18) we get:

$$\begin{aligned} &\frac{dV(t)}{dt} = \frac{dV_\omega(t)}{dt} + \frac{dV_\varphi(t)}{dt} = s_\omega(t)\dot{s}_\omega(t) + s_\varphi(t)\dot{s}_\varphi(t) \\ &\frac{dV(t)}{dt} == -\left\{\beta_1 s_\omega(t)\left[K_{p\omega} e_\omega(t) + K_{I\omega}\int_0^t e_\omega(t)dt + u_{\omega \mathrm{AST}A}(t)\right]\right. \\ &\left. +\beta_2 s_\varphi(t)\left[K_{p\varphi} e_\varphi(t) + K_{I\varphi}\int_0^t e_\varphi(t)dt + u_{\varphi \mathrm{AST}A}(t)\right]\right\};\ \beta_{1:2} > 0 \end{aligned} \tag{22}$$

If $e_m(t) > 0$, from (7) and (15) we have $s_m(t) > 0$, combining (12), (13), (18), and (19) we have $\dot{s}_m(t) < 0$. Therefore $\frac{dV(t)}{dt} < 0$. If $e_m(t) < 0$, from (7) and (15) we have $s_m(t) < 0$, combining (12), (13), (18) and (19) we have $\dot{s}_m(t) > 0$. Therefore $\frac{dV(t)}{dt} < 0$. From (22) we have: $\frac{dV(t)}{dt} < 0 \forall e_m(t);\ m = \omega{:}\varphi$. Thus, the system is always stable according to Lyapunov stability theory.

4. RESULTS AND DISCUSSION

The effectiveness of the proposed hybrid PI–ASTA_NTSMC scheme was examined in MATLAB/Simulink 2023b using a squirrel-cage induction motor model. The motor specifications are: 400 V, 50 Hz, 2 pole, 2880 rpm, Rs = 1.97 Ω, Rr = 1.96 Ω, Ls = 0.0154 H, Lr = 0.0154 H, Lm = 0.3585H, J = 0.00242 kg.m^2, B = 0.0005. The complete simulation structure is depicted in Figure 1.

4.1. Dynamic performance evaluation under rated load moment

Figure 2 and Table 1 present the comparative dynamic responses of the conventional PI, PI–FOSMC, and the proposed hybrid PI–ASTA–NTSMC controllers under rated load conditions. As observed, the proposed hybrid controller achieves the fastest transient and most accurate steady-state performance among all schemes. Quantitatively, the settling time is reduced from 0.0671 s (PI) and 0.0594 s (PI–FOSMC) to 0.0407 s, representing improvements of 39.4% and 31.5%, respectively. The overshoot is nearly eliminated, decreasing from 0.6634 rad/s (PI) and 0.3834 rad/s (PI–FOSMC) to only 0.0091 rad/s with the proposed approach. These substantial improvements in transient behavior arise from the finite-time convergence property of the NTSMC surface and the higher-order continuity of the adaptive super-twisting algorithm (ASTA), which together suppress oscillations and mitigate the chattering phenomenon inherent to conventional sliding-mode drives. Moreover, the ISE (0.0035) and IAE (0.0256) indices of the proposed controller are considerably smaller than those of PI (0.0473, 0.1105) and PI–FOSMC (0.0049, 0.0337), confirming that the overall tracking-error energy is minimized.

In addition to improved speed regulation, Figure 2 shows that the Hybrid PI–ASTA–NTSMC also yields a much smoother and more stable rotor-flux trajectory. Whereas the PI and PI–FOSMC controllers exhibit noticeable flux oscillations and coupling effects during acceleration and deceleration, the proposed strategy maintains an almost constant flux magnitude with negligible ripple. This enhanced flux regulation, enabled by the hybrid PI–ASTA–NTSMC flux loop, ensures finite-time flux convergence and effectively compensates for inverter nonlinearities and magnetic saturation. As a result, torque production remains linear, torque ripple is reduced, and current stress is minimized. Consequently, the RMSE of speed and torque decreases to 0.1156 and 0.1775, corresponding to improvements of over 72% in speed accuracy and 16% in torque smoothness compared with PI control. Overall, the dual-loop hybrid structure enables well-coordinated torque–flux decoupling and delivers rapid transient recovery with minimal ripple, consistent with the stability analysis in section 3.

From the obtained survey results, it is easy to see that the proposed structure provides a smoother and more energy-efficient control effort. The continuous higher-order ASTA formulation generates bounded control derivatives, which significantly reduces high-frequency switching activity compared with PI–FOSMC. This behavior not only mitigates chattering but also decreases voltage stress and thermal loading on the inverter power devices. Additionally, the controller is more resistant to noise caused by digital sampling. Since the ASTA term avoids a pure sign function and instead uses a continuous approximation, quantization and sampling jitter are effectively filtered out. This makes the controller highly suitable for real-time DSP implementation, where limited sampling rates and digital noise often degrade first-order sliding mode schemes. From a computational perspective, the hybrid PI–ASTA–NTSMC algorithm maintains a lightweight arithmetic structure. Its per-cycle computational load is comparable to PI–FOSMC and far lower than advanced predictive or ANN-based controllers, ensuring full compatibility with low-cost TI C2000 processors.

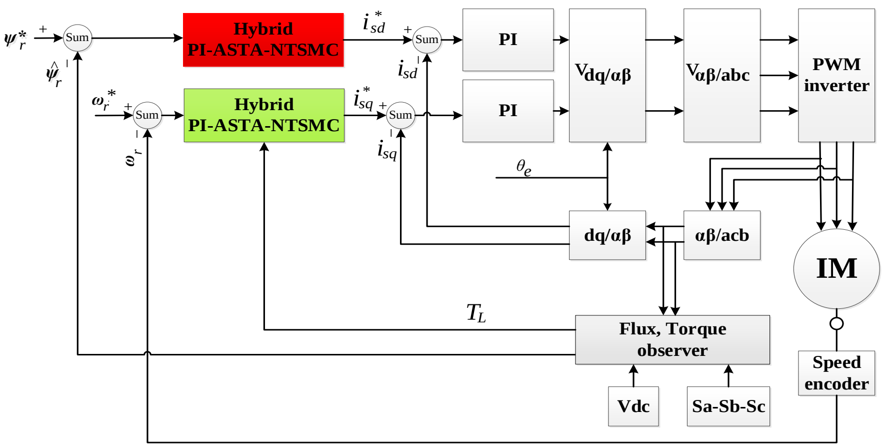

Figure 1. Simulation model of hybrid PI-ASTA-NTSMC algorithm based FOC

Table 1. Indices for evaluating control performance

Control strategy	Settling time	Overshoot	ISE	IAE	RMSE speed	RMSE torque
PI control	0.0671	0.6634	0.0473	0.1105	0.4265	0.2119
PI-FOSMC	0.0594	0.3834	0.0049	0.0337	0.1377	0.2065
PI-ASTANTSMC	0.0407	0.0091	0.0035	0.0256	0.1156	0.1775

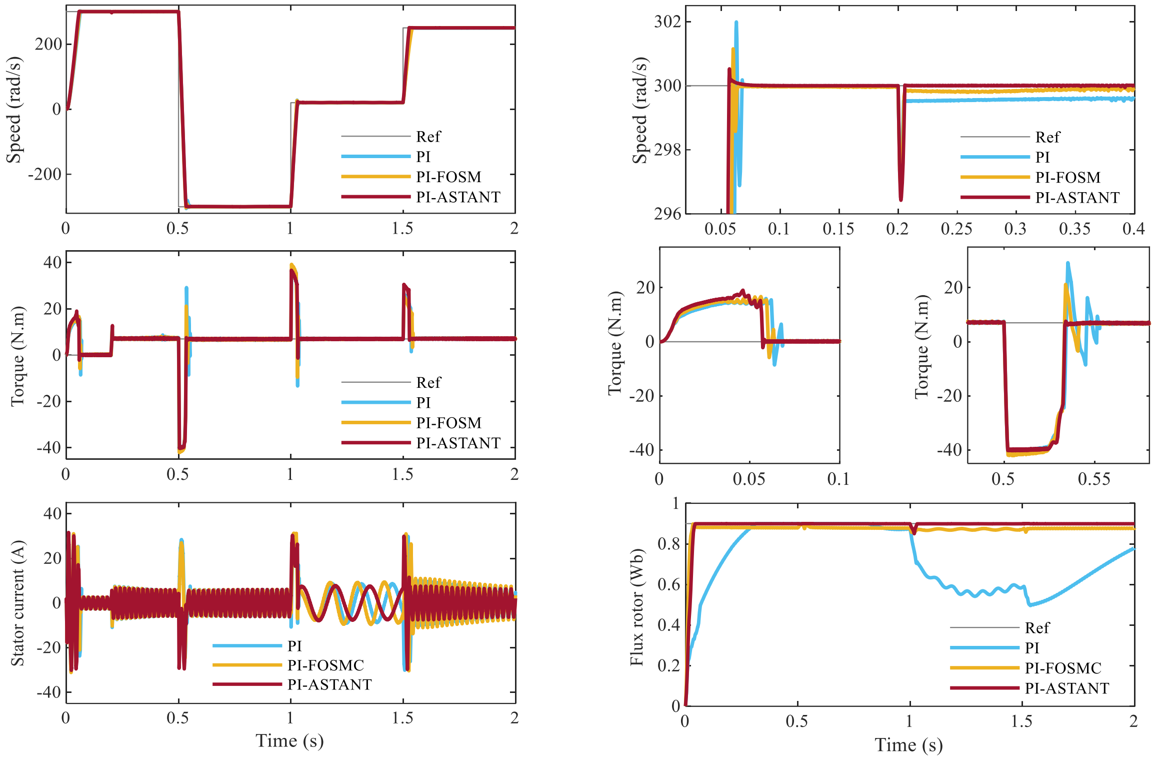

Figure 2. Performance of PI, PI-FOSMC, and hybrid PI-ASTA_NTSMC under the variable speed

4.2. Robustness evaluation under load disturbance

The robustness of the proposed controller was further evaluated under sudden load torque variations, as shown in Figure 3. Under a step disturbance, the conventional PI controller exhibits large speed deviations and prolonged recovery, indicating weak disturbance rejection capability. The PI–FOSMC improves resilience by enforcing a sliding mode, but the fixed-gain switching induces observable chattering in both speed and electromagnetic torque. By contrast, the Hybrid PI–ASTA–NTSMC exhibits superior robustness and fast disturbance rejection. When the external load torque abruptly changes, the adaptive ASTA mechanism instantly increases its switching gain to counteract the disturbance, ensuring the sliding variable quickly converges to zero. As the transient subsides, the adaptive law smoothly reduces the control gain, thereby maintaining continuous control and effectively suppressing chattering. This dynamic gain adaptation results in finite-time recovery of the speed to its reference within a negligible deviation of ±0.5%, while the electromagnetic torque rapidly stabilizes without overshoot.

Furthermore, the rotor flux remains tightly regulated during the entire disturbance period, indicating strong flux decoupling and effective compensation of magnetic cross-coupling effects. This stable flux profile contributes to consistent torque generation and reduced stator current stress, further demonstrating the synergy between the speed and flux control loops. Compared with PI, PI–FOSMC, the hybrid controller reduces both torque ripple and integral of absolute error (IAE) significantly, confirming its adaptive and disturbance-tolerant characteristics. In addition, the sliding-mode structure embedded in the ASTA–NTSMC framework inherently strengthens robustness against matched disturbances such as load torque variations. Because load torque enters the mechanical dynamics through the same channel as the control input, the sliding-mode term naturally compensates for this disturbance once the system reaches the sliding surface. This means that the proposed controller can reject sudden or sustained load variations without requiring explicit disturbance estimation. The combination of a nonsingular terminal sliding surface and an adaptive super-twisting law ensures that the system is driven toward the sliding manifold in finite time and remains insensitive to load perturbations, modeling inaccuracies, and parameter drift. These results clearly demonstrate that the proposed hybrid controller integrates adaptive robustness and smooth control effort within a single framework, allowing the IM drive to maintain stable performance even under severe load disturbances.

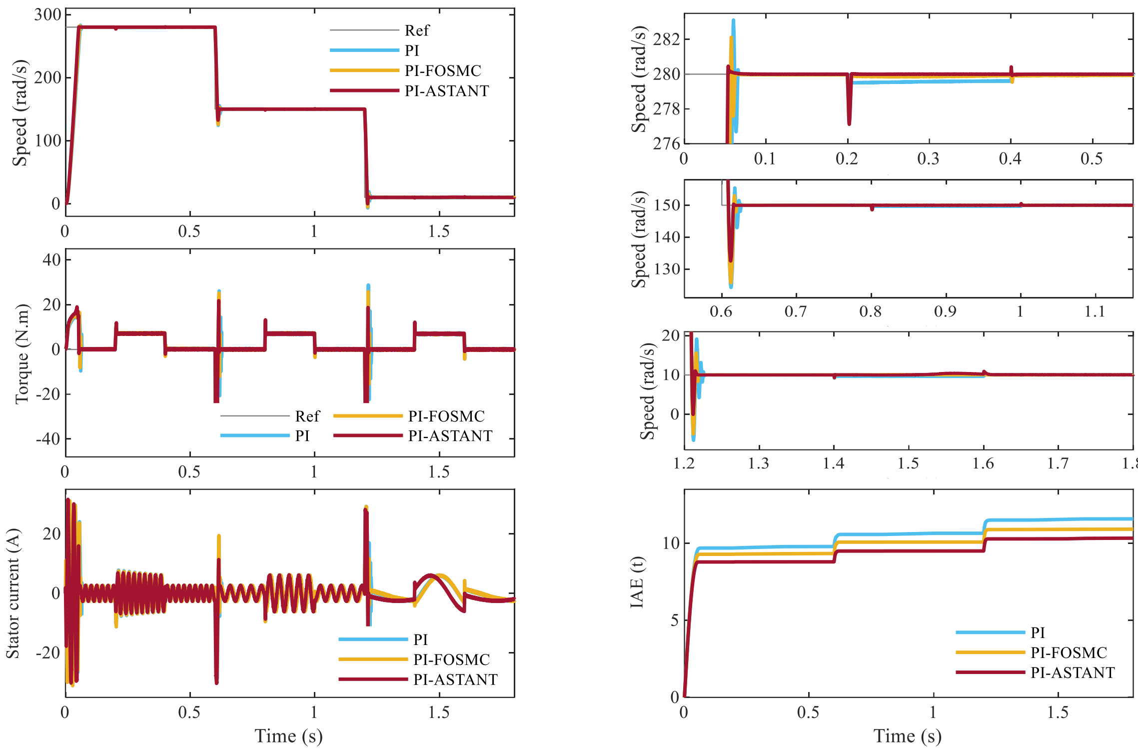

Figure 3. Performance of PI, PI-FOSMC, and hybrid PI-ASTA_NTSMC under the variable torque

4.3. Robustness evaluation under parameter variations (resistance changes)

In this robustness test, the load torque was kept constant at its rated value of 7 N.m, while the rotor resistance was increased by 200% at the beginning of the simulation. Because rotor resistance R_r has a dominant influence on flux dynamics, torque production, and the overall stability of the induction motor control loop—much greater than the weaker, secondary effects of stator resistance R_s only R_r variation is considered in this robustness survey. This condition emulates severe thermal stress or degradation of the rotor cage, which shortens the rotor time constant and directly influences the flux–torque coupling and electromagnetic dynamics of the induction motor. As shown in Figure 4, the conventional PI and PI–FOSMC controllers exhibit substantially degraded performance in the high-speed operating range: both controllers show large steady-state speed error and elevated speed error energy, with correspondingly higher RMSE values and increased torque ripple. These degradations are consistent with reduced torque production capability at a fixed current when the rotor time constant is shortened. In contrast, the hybrid PI–ASTA–NTSMC controller maintains excellent performance despite the 200% rotor-resistance increase. Owing to the adaptive ASTA law, the control gain automatically rises during transient flux deviation and smoothly decreases once the sliding variable approaches zero, ensuring finite-time convergence of both speed and flux without inducing chattering. The rotor flux trajectory remains nearly constant and well-decoupled from the torque channel, preserving linear electromagnetic torque production. Consequently, the torque waveform exhibits minimal ripple and negligible offset even under the elevated rotor resistance, while the speed response closely tracks its reference with the smallest ISE, IAE, and RMSE values among all compared schemes.

Furthermore, because the rotor flux magnitude is effectively maintained, the stator current amplitude remains stable, preventing excessive copper loss or overheating. This demonstrates that the hybrid controller not only sustains precise speed and torque control under severe parameter variation but also preserves current efficiency and thermal reliability of the drive. These results confirm the theoretical robustness analysis presented in section 3, where adaptive gain modulation and nonsingular terminal sliding ensure global finite-time stability and parameter insensitivity. Overall, the proposed Hybrid PI–ASTA–NTSMC achieves superior parameter robustness, reduced torque ripple, and enhanced flux–torque linearity compared with conventional PI and PI–FOSMC controllers.

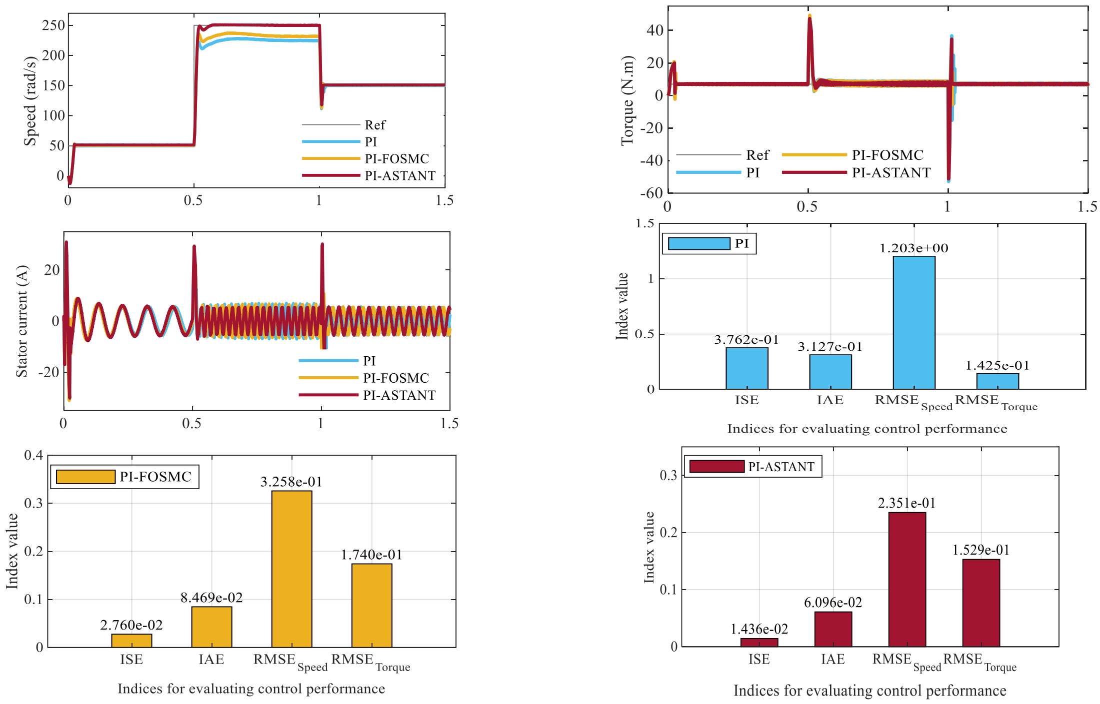

Figure 4. Performance of PI, PI-FOSMC, and hybrid PI-ASTA_NTSMC under the variations resistances

5. CONCLUSION

This paper has proposed a novel hybrid PI–ASTA–NTSMC control scheme for high-performance induction motor drives (IMDs). The hybrid architecture combines the steady-state accuracy of a PI regulator with the adaptive robustness of a super-twisting sliding mode controller defined on a nonsingular terminal sliding surface. The ASTA mechanism dynamically tunes switching gains, ensuring finite-time convergence, strong disturbance rejection, and chattering suppression. A Lyapunov-based analysis confirmed the finite-time stability of the closed loop. Simulation results under three representative scenarios—wide-speed operation with rated load, sudden load disturbances, and a 200% rotor-resistance increase at a constant 7 N.m load—validated the controller's superiority. The proposed scheme reduced the settling time to 0.0407 s, achieving 39.4% and 31.5% improvements over PI and PI–FOSMC, while almost eliminating overshoot (0.0091 rad/s) and minimizing ISE, IAE, and RMSE indices. Even under severe parameter variation, it maintained accurate speed tracking and stable torque, whereas conventional methods exhibited significant degradation at high speeds.

However, the current validation is restricted to MATLAB/Simulink simulations, and practical aspects such as inverter nonlinearities, measurement noise, sampling limitations, computational load, and actuator saturation have not yet been examined. As future work, we plan to implement the proposed controller on a real-time TI C2000 platform and perform hardware-in-the-loop (HIL) and laboratory experiments on an actual induction motor drive. These efforts will enable a more complete assessment of industrial feasibility and verify the controller's robustness under real operating conditions. Overall, the hybrid PI–ASTA–NTSMC approach provides a balanced solution that unites theoretical rigor with practical applicability. With its adaptive gain mechanism, finite-time convergence, and chattering-free behavior, the proposed controller remains a computationally efficient and promising solution for precision industrial drives.

FUNDING INFORMATION

Authors state no funding involved.

AUTHOR CONTRIBUTIONS STATEMENT

This journal uses the Contributor Roles Taxonomy (CRediT) to recognize individual author contributions, reduce authorship disputes, and facilitate collaboration.

Name of Author	C	M	So	Va	Fo	I	R	D	O	E	Vi	Su	P	Fu
Duc Thuan Le		✓	✓	✓	✓			✓	✓				✓	
Ngoc Thuy Pham	✓					✓	✓	✓		✓	✓	✓		

C : **C**onceptualization
M : **M**ethodology
So : **So**ftware
Va : **Va**lidation
Fo : **Fo**rmal analysis
I : **I**nvestigation
R : **R**esources
D : **D**ata Curation
O : Writing - **O**riginal Draft
E : Writing - Review & **E**diting
Vi : **Vi**sualization
Su : **Su**pervision
P : **P**roject administration
Fu : **Fu**nding acquisition

CONFLICT OF INTEREST STATEMENT

The authors declare that there is no conflict of interest regarding the publication of this paper.

DATA AVAILABILITY

The data that support the findings of this study are available from the corresponding author, [NP], upon reasonable request.

REFERENCES

[1] E. Rosas, C. Bórquez, D. Barria, S. Ojeda, J. Rohten, and J. Silva, "Comparison of control strategies for induction motors: indirect field oriented control, direct torque control and predictive torque control," in *2024 IEEE International Conference on Automation/XXVI Congress of the Chilean Association of Automatic Control (ICA-ACCA)*, Oct. 2024, pp. 1–6. doi: 10.1109/ICA-ACCA62622.2024.10766770.

[2] Himani, S. V. S. P. K. Ch, S. Venu, and S. Jain, "Robust and motor parameter insensitive PI controller design for field-oriented controlled induction motor drive," *International Journal of Circuit Theory and Applications*, Jul. 2025, doi: 10.1002/cta.70042.

[3] W. Song, J. Li, C. Ma, Y. Xia, and B. Yu, "A simple tuning method of PI regulators in FOC for PMSM drives based on deadbeat predictive conception," *IEEE Transactions on Transportation Electrification*, vol. 10, no. 4, pp. 9852–9863, Dec. 2024, doi: 10.1109/TTE.2024.3385114.

[4] L. Ouboubker, J. Lamterkati, M. Khafallah, and A. El Afia, "Real time implementation of anti-windup PI controller for speed control of induction machine based on DTC strategy," *International Journal of Power Electronics and Drive Systems (IJPEDS)*, vol. 12, no. 3, pp. 1358–1368, Sep. 2021, doi: 10.11591/ijpeds.v12.i3.pp1358-1368.

[5] M. S. Kumar, G. Satheesh, and P. Sujatha, "Optimal PI controller parameter setting for torque ripple minimization in SVPWM–DTC based BLDC motor drive using sine cosine algorithm," *Engineering Research Express*, vol. 6, no. 4, p. 045359, Dec. 2024, doi: 10.1088/2631-8695/ad9c14.

[6] W. Yu, K. Zhu, and Y. Yu, "Variable universe fuzzy PID control for active suspension system with combination of chaotic particle swarm optimization and road recognition," *IEEE Access*, vol. 12, pp. 29113–29125, 2024, doi: 10.1109/ACCESS.2024.3368762.

[7] S. Wang, C. Jiang, Q. Tu, H. Shu, and C. Zhu, "Particle swarm optimization of fuzzy PI control for PMSMs," *Journal of Power Electronics*, vol. 23, no. 10, pp. 1585–1593, Oct. 2023, doi: 10.1007/s43236-023-00643-x.

[8] M. A. Hossain and M. Shahjahan, "Memoryless radial basis function neural network based proportional integral controller for PMSM drives," *International Journal of Power Electronics and Drive Systems (IJPEDS)*, vol. 14, no. 1, pp 89–99, Mar. 2023, doi: 10.11591/ijpeds.v14.i1.pp89-99.

[9] H. Jie, G. Zheng, J. Zou, X. Xin, and L. Guo, "Adaptive decoupling control using radial basis function neural network for permanent magnet synchronous motor considering uncertain and time-varying parameters," *IEEE Access*, vol. 8, pp. 112323–112332, 2020, doi: 10.1109/ACCESS.2020.2993648.

[10] H. Rafia, H. Ouadi, F. Giri, and B. El Bhiri, "Advanced hybrid control for induction motor combining ANN-PID speed controller with neural predictive current regulator based on particle swarm optimization," *Transactions of the Institute of Measurement and Control*, vol. 47, no. 7, pp. 1387–1402, Apr. 2025, doi: 10.1177/01423312241277246.

[11] J. Fei and Y. Chen, "Dynamic terminal sliding-mode control for single-phase active power filter using new feedback recurrent neural network," *IEEE Transactions on Power Electronics*, vol. 35, no. 9, pp. 9904–9922, Sep. 2020, doi: 10.1109/TPEL.2020.2974470.

[12] P. Proaño, R. Díaz, C. Chillán, J. Medina, W. Chamorro, and J. Zuñiga, "Sliding mode control proposed using a Clegg integrator for speed control of a three-phase induction motor," in *Engineering Proceedings*, Nov. 2024, vol. 77, no. 1, p. 8, doi: 10.3390/engproc2024077008.

[13] L. Fridman, A. Poznyak, and F. J. Bejarano, *Robust output LQ optimal control via integral sliding modes*. New York, NY: Springer New York, 2014, doi: 10.1007/978-0-8176-4962-3.

[14] M. Rubagotti, A. Estrada, F. Castanos, A. Ferrara, and L. Fridman, "Integral sliding mode control for nonlinear systems with matched and unmatched perturbations," *IEEE Transactions on Automatic Control*, vol. 56, no. 11, pp. 2699–2704, Nov. 2011, doi: 10.1109/TAC.2011.2159420.

[15] X. Xiong, H. Chen, Y. Lou, Z. Liu, S. Kamal, and M. Yamamoto, "Implicit discrete-time adaptive first-order sliding mode control with predefined convergence time," *IEEE Transactions on Circuits and Systems II: Express Briefs*, vol. 68, no. 12, pp. 3562–3566, Dec. 2021, doi: 10.1109/TCSII.2021.3070435.

[16] J. Hong, X. Lin, J. Zhang, W. Huang, B. Yan, and X. Li, "A composite sliding mode control with the first-order differentiator and sliding mode observer for permanent magnet synchronous machine," *ISA Transactions*, vol. 147, pp. 489–500, Apr. 2024, doi: 10.1016/j.isatra.2024.02.006.

[17] N. T. Pham, "Design of novel STASOSM controller for FOC control of dual star induction motor drives," *International Journal of Robotics and Control Systems*, vol. 4, no. 3, pp. 1059–1074, Jun. 2024, doi: 10.31763/ijrcs.v4i3.1443.

[18] S. Ding, Q. Hou, and H. Wang, "Disturbance-observer-based second-order sliding mode controller for speed control of PMSM drives," *IEEE Transactions on Energy Conversion*, vol. 38, no. 1, pp. 100–110, Mar. 2023, doi: 10.1109/TEC.2022.3188630.
[19] X. Lin, B. Zhang, S. Fang, R. Xu, S. Guo, and J. Liu, "Adaptive generalized super twisting sliding mode control for PMSMs with filtered high-gain observer," *ISA Transactions*, vol. 138, pp. 639–649, Jul. 2023, doi: 10.1016/j.isatra.2023.02.008.
[20] H. Benderradji, S. Benaicha, and L. C. Alaoui, "Improved sliding mode control for induction motor based on twisting algorithm," *AIMS Electronics and Electrical Engineering*, vol. 9, no. 1, pp. 81–98, 2025, doi: 10.3934/electreng.2025005.
[21] Y. Tian, Y. Cai, and Y. Deng, "A fast nonsingular terminal sliding mode control method for nonlinear systems with fixed-time stability guarantees," *IEEE Access*, vol. 8, pp. 60444–60454, 2020, doi: 10.1109/ACCESS.2020.2980044.
[22] Y. Yan, T. Jin, X. Yu, S. Yu, and G. Guo, "Event-triggered nonsingular terminal sliding-mode control," *IEEE Transactions on Cybernetics*, vol. 55, no. 7, pp. 3356–3367, Jul. 2025, doi: 10.1109/TCYB.2025.3553898.
[23] B. Xu, L. Zhang, and W. Ji, "Improved non-singular fast terminal sliding mode control with disturbance observer for PMSM drives," *IEEE Transactions on Transportation Electrification*, vol. 7, no. 4, pp. 2753–2762, Dec. 2021, doi: 10.1109/TTE.2021.3083925.
[24] X. Li, J. Liu, Y. Yin, and K. Zhao, "Improved super-twisting non-singular fast terminal sliding mode control of interior permanent magnet synchronous motor considering time-varying disturbance of the system," *IEEE Access*, vol. 11, pp. 17485–17496, 2023, doi: 10.1109/ACCESS.2023.3244190.
[25] D. Xu, B. Ding, B. Jiang, W. Yang, and P. Shi, "Nonsingular fast terminal sliding mode control for permanent magnet linear synchronous motor via high-order super-twisting observer," *IEEE/ASME Transactions on Mechatronics*, vol. 27, no. 3, pp. 1651–1659, Jun. 2022, doi: 10.1109/TMECH.2021.3086527.
[26] D. Shi, K. Bodemann, Y. Wang, C. Xu, L. Liu, and C. Feng, "A novel nonsingular fast terminal sliding mode control with sliding mode disturbance observer for permanent magnet synchronous motor servo control," *Processes*, vol. 12, no. 9, p. 1986, Sep. 2024, doi: 10.3390/pr12091986.
[27] D. Fu, X. Zhao, and H. Yuan, "Nonsingular terminal sliding mode control based on adaptive time delay estimation for permanent magnet linear synchronous motor," *International Journal of Control, Automation and Systems*, vol. 20, no. 1, pp. 24–34, Jan. 2022, doi: 10.1007/s12555-020-0448-z.
[28] P. Krause, O. Wasynczuk, S. Sudhoff, and S. Pekarek, *Analysis of electric machinery and drive systems*. 3rd ed. Hoboken, NJ, USA: Wiley-IEEE Press, 2013.

BIOGRAPHIES OF AUTHORS

Duc Thuan Le is a lecturer in the Department of Electrical Engineering Technology, Industrial University of Ho Chi Minh City (IUH), Ho Chi Minh, Viet Nam. He received the B.Sc. degree in electrical engineering from Thai Nguyen University of Technology in 1994 and the M.Sc. degree in control engineering and automation from Ha Noi University of Transport in 2020. His research interests include the field of power electronics, intelligent control, multiphase induction motor, AC motor drives, and embedded systems. He can be contacted at email: leducthuan@iuh.edu.vn.

Ngoc Thuy Pham is a lecturer in the Department of Electrical Engineering Technology, Industrial University of Ho Chi Minh City (IUH), Ho Chi Minh, Viet Nam. She received the B.Sc. and M.Sc. degrees in electrical engineering from Thai Nguyen University of Technology in 1994 and Ho Chi Minh City University of Technology (HCMUT) in 2009, respectively, and a Ph.D. degree in control engineering and automation from TE and Electrical Engineering from Ho Chi Minh City University of Transport, in 2020. Her current research interests include power electronics, AC motor drives, intelligent control, multiphase induction motor, sensorless control of multiphase induction motor drives, and embedded systems. She can be contacted at email: phamthuyngoc@iuh.edu.vn.